Chinese Journal of Oceanology and Limnology
Vol. 31 No. 2, P. 334-344, 2013
http://dx.doi.org/10.1007/s00343-013-2109-z

Numerical modeling of hydrodynamic changes due to coastal reclamation projects in Xiamen Bay, China*

WANG Jia (王佳)[1], HONG Huasheng (洪华生)[1], ZHOU Lumin (周鲁闽)[2], HU Jianyu (胡建宇)[1], JIANG Yuwu (江毓武)[1, **]

[1] *State Key Laboratory of Marine Environmental Science*, *Xiamen University*, *Xiamen 361005*, *China*

[2] *Ocean & Fisheries Bureau of Xiamen*, *Xiamen 361012*, *China*

Received May 24, 2012; accepted in principle Jun. 19, 2012; accepted for publication Jun. 28, 2012

© Chinese Society for Oceanology and Limnology, Science Press, and Springer-Verlag Berlin Heidelberg 2013

Abstract Xiamen Bay in South China has experienced extensive coastal exploitation since the 1950s, resulting in some severe environmental problems. Local authorities now have completed or are implementing many environmental restoration projects. Evaluating the cumulative impact of exploitation and restoration activities on the environment is a complicated multi-disciplinary problem. However, hydrodynamic changes in the bay caused by such coastal projects can be characterized directly and definitively through numerical modeling. This paper assesses the cumulative effect of coastal projects on the hydrodynamic setting using a high-resolution numerical modeling method that makes use of tidal current speeds and the tidal prism as two hydrodynamic indices. Changes in tidal velocity and the characteristics of the tidal prism show that hydrodynamic conditions have declined from 1938 to 2007 in the full-tide area. The tidal current speed and tidal prism have decreased by 40% in the western part of the bay and 20% in the eastern part of the bay. Because of the linear relationship between tidal prism and area, the degraded hydrodynamic conditions are anticipated to be restored to 1972 levels following the completion of current and proposed restoration projects, i.e. 33% and 15% decrease in the hydrodynamic conditions of 1938 for the western and eastern parts of the bay, respectively. The results indicate that hydrodynamic conditions can be restored to some extent with the implementation of a sustainable coastal development plan, although a full reversal of conditions is not possible. To fully assess the environmental changes in a region, more indices, e.g., water quality and ecosystem parameters, should be considered in future evaluations.

Keyword: coastal exploitation; numerical model; hydrodynamic conditions; project assessment

1 INTRODUCTION

Hydrodynamic conditions are key environmental factors in coastal zones. Hydrodynamic conditions determine the water exchange capacity, which is directly related to water quality, and therefore greatly affect coastal economic development. For example, deposition caused by weak currents along a maritime transport route will greatly inhibit shipping and commerce. In coastal regions, local hydrodynamic conditions can be changed by various human activities including those associated with economic and urban development. Since the 1950s, there has been extensive coastal development in the Xiamen Bay region of China, including land reclamation, dike construction and harbor building.

Xiamen Bay, one of the largest harbors in China, is located on the west side of the Taiwan Strait. For convenience, it can be divided into four regions: the Jiulong River estuary, western and eastern 'sub-bays', and the adjacent sea area to the south in the vicinity of Xiamen Island (Fig.1a). Average water depth varies from 30 m in shipping routes to negative values in intertidal zones. Xiamen Bay has a semi-diurnal tide that propagates into the bay from the south and east of Kinmen Island. The maximum tidal range and current

* Supported by the National Natural Science Foundation of China (Nos. 41076001, 40810069004) and the Fundamental Research Funds for the Central Universities (No. 2010121029)

** Corresponding author: ywjiang@xmu.edu.cn

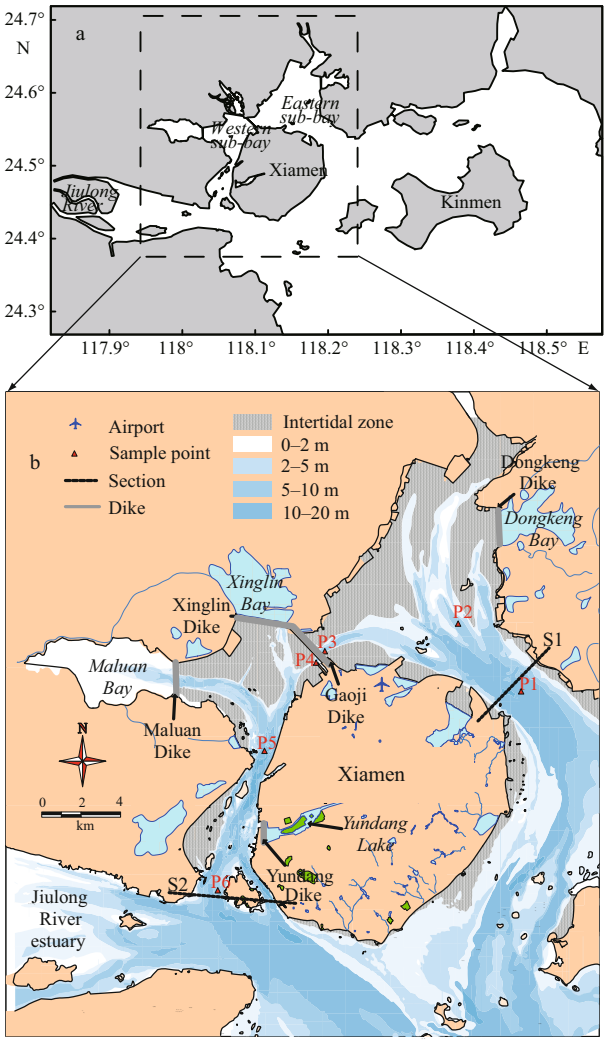

Fig.1 Geographical location of the study area. a. model domain containing the nested domain (dashed line); b. coastline and place names of Xiamen Bay valid for 2007 along with the distribution of sample points and sections

speed can reach 6 m and 1.5 m/s, respectively. The intense hydrodynamic processes provided by the tide assist in the maintenance of shipping routes and marine water quality. The western and eastern sub-bays are the closest ocean economic zones to the city of Xiamen, and correspondingly their hydrodynamic conditions and water quality have been influenced significantly by human activities.

Different indices have been used in environmental impact assessments of coastal projects, e.g., water elevation, speed at key points, tidal prism, water exchange rate, sediment deposits and water quality (Wang et al., 2000; Qin et al., 2002; Zhao et al., 2002; Jiang et al., 2004a; Wu and Chau, 2006; Xia et al., 2006; Zhao et al., 2006; Guo et al., 2007; Zheng et al., 2007). Recently, modeling-based ecological studies have also been applied in evaluations of the coastal environment (Chau, 2005; Muttil and Chau, 2006). In general, hydrodynamic change is the main focus of such studies because of its control on pollution capacity and deposition rate in navigable channels. Normally, the tidal current and prism are the main physical constraints on the water exchange rate and pollutant capacity of the bay. These two factors are of major interest to local authorities and are taken as the primary indices in environmental impact assessments of coastal projects in the region. Hence, we have also selected tidal current speed and tidal prism as the indices of hydrodynamic conditions for this study. In the following sections, we present the use of a numerical modeling method to study the hydrodynamic changes of the western and eastern sub-bays of Xiamen Bay.

The history of coastal development and reclamation in Xiamen Bay can be divided into two periods or phases. During the first phase, from the 1950s to the 1980s, numerous large reclamation and dike construction projects were undertaken for the benefit of ship traffic and agriculture. These projects greatly changed the coastline, as shown in Fig.1b. For example, in 1956 the 2 122-m-long and 20-m-wide Gaoji Dike was built to provide a convenient railroad transportation route between the Chinese mainland and Xiamen Island (Cheng et al., 1985). However, the dike cut off water flow between the western and eastern sub-bays. Xinglin, Maluan, and Yundang bays (with areas of 20.00, 20.93 and 6.70 km^2, respectively) have been separated from the western sub-bay by the dikes for the purpose of aquaculture. Yundang Bay was renamed Yundang Lake after the completion of this project and urban construction began along the shores. Similarly, in the eastern sub-bay, a large number of reclamations converted the beach at the north into land for agriculture or other purposes. For example, Dongkeng Bay was separated by a dike to produce a salt field with an area of 7.3 km^2. The second phase of coastal development occurred from the 1980s to the 2000s. In this phase, the scale of the reclamation was smaller and the objective switched to the development of real estate, harbors, and airport. These reclamations led to a significant decrease in sea area of Xiamen Bay. For example, in 1938, the western and eastern sub-bays had areas of 101 and 120 km^2, respectively. By 2007, these areas had shrunk to 45 and 88 km^2 (Table 1). As a result, the hydrodynamics and environmental carrying capacity

of the marine environment decreased substantially, which introduced a myriad of problems that hampered nearby urban development. For example, the sediment deposition rate in the shipping route can be as high as 0.3 m/year at the mouth of the western sub-bay, requiring annual dredging to ensure safe navigation. Additionally, the water quality decreased to a highly polluted level, as indicated by the index of inorganic nitrogen, and water blooms occurred several times each year (Xiamen Municipal Government, P. R. China, 2005–2008).

To improve the quality of the marine environment and encourage sustainable development, a series of environmental restoration projections were proposed by experts and managers. All of these projects are now ongoing and planned for completion in 2013. The main projects related to the hydrodynamics of the area are:

1. Opening an 800-m-long stretch of the Gaoji Dike, using a bridge to span the opening, to enhance water exchange between the western and eastern sub-bays.

2. Opening gaps in the Maluan, Xinglin and Dongkeng Dikes by 200, 250 and 700 m, respectively, to increase the hydrodynamic conditions in the western sub-bay.

3. Dredging the deposited mud in the western and eastern sub-bays to the level of low slack tide, to increase the tidal prism and enhance the hydrodynamic conditions.

Although almost every coastal project in Xiamen Bay had been individually simulated by numerical modeling to provide information on anticipated hydrodynamic changes, this paper studies the accumulated effect of 70 year of coastal projects with the use of a high resolution (approximately 35 m) nested numerical model. Moreover, the degree of recovery in the hydrodynamic conditions made possible by the restoration projects in the bay is discussed.

2 MODEL AND METHOD

2.1 Model description

A modified two-dimensional (2-D) modeling method based on the external mode of a Princeton Ocean Model (POM) (Blumberg and Mellor, 1987) is used in this study. The modified modeling scheme includes a stable method for the drying and wetting processes (Jiang and Wai, 2005) and a two-way nested grid technique (Oey and Chen, 1992) that can represent water processes in a large tidal flat area and complex coastline (the area is indicated by a gray shadow in Fig.1b). In addition, the Alternating Direction Implicit method (Leedertse, 1970) was adopted to handle the 2-D module in this model with an implicit scheme, guaranteeing a larger time step without being restricted by the Courant-Friendrichs-Levy calculation stability condition (Chau and Jiang, 2001). A Geographic Information System (GIS) technique was used for pre/post-processing to enhance the modeling accuracy and visibility (Jiang et al., 2004b).

Table 1 Tidal area of the four cases (unit: km^2)

Case	Western sub-bay	Eastern sub-bay
Case 1 (1938)	101.50	120.00
Case 2 (1984)	54.23	97.46
Case 3 (2007)	45.62	88.63
Case 4 (2012)	58.79	84.22

2.2 Model domain and simulated cases

In Fig.1a, all four modeled domains have a coarse grid resolution of approximately 250 m; this includes all of Xiamen Bay and the nearby sea. To resolve the complex topography and coastline of the western and eastern sub-bays, a nested sub-domain (dashed box) is used with a grid resolution of approximately 35 m. Using the reclamation history and available sea charts, we simulated and evaluated the hydrodynamic state in 1938 (Case 1), 1984 (Case 2), 2007 (Case 3) and 2012 (Case 4, after the completion of restoration projects). The coastlines of Xiamen Bay for all four cases are shown in the upper panel of Fig.2. The coastline of Xiamen Bay changed significantly from 1938 to 1984, corresponding to the first reclamation phase mentioned in section 1. The main purpose of the reclamation areas prior to 1984 was agriculture. From 1984 to 2007, reclamations were undertaken for the harbor, airport and real estate construction, corresponding to a phase of rapid economic development in Xiamen. The restoration projects (e.g., partially opening the dikes in Maluan, Xinglin and Dongkeng Bays) and sludge dredging are now ongoing. The bottom panel in Fig.2 shows the fine and nested grids that suitably represent the land boundaries of the four presented cases.

2.3 Model configuration

Coastline and topography data have been digitized from navigation charts published by China's Maritime

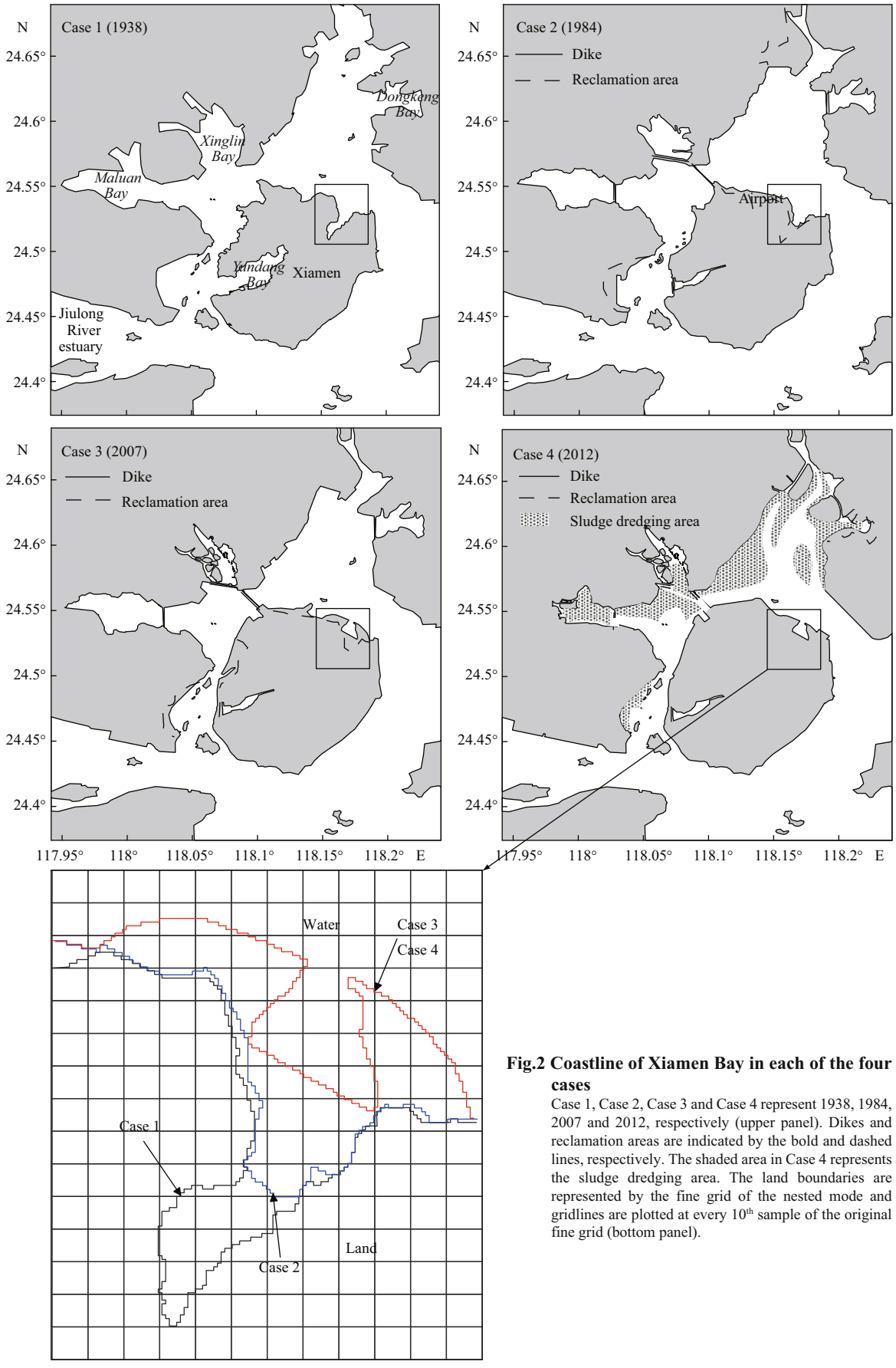

Fig.2 Coastline of Xiamen Bay in each of the four cases

Case 1, Case 2, Case 3 and Case 4 represent 1938, 1984, 2007 and 2012, respectively (upper panel). Dikes and reclamation areas are indicated by the bold and dashed lines, respectively. The shaded area in Case 4 represents the sludge dredging area. The land boundaries are represented by the fine grid of the nested mode and gridlines are plotted at every 10th sample of the original fine grid (bottom panel).

Safety Administration. The grid numbers are 320×200 in the coarsely-sampled domains and 839×930 in the finely-sampled sub-domains. The southern and eastern open boundaries were forced by the tidal elevation which was calculated using the harmonic constants of sixteen component tides (K_1, K_2, O_1, M_2, S_2, $2N_2$, J_1, L_2, M_1, MU_2, N_2, NU_2, OO_1, P_1, Q_1, and T_2) available from the tidal dataset Nao. 99b (version 2000.09.09) (Matsumoto et al., 2000). In the nested domain, the variables (e.g., elevation and velocity) at the boundary were interpolated from the model domain. The value of the model domain inside the nested domain was replaced with values from the nested domain, forming a two-way nested modeling scheme. For the purpose of comparison, the four cases were calculated for the same spring tidal process (GMT+8 2007/8/14 12:00–2007/8/15 14:00). The time step was set to 60 s for both the coarse and fine grids. The average annual runoff of the Jiulong River of approximately 321 m^3/s was added into each model as a point source. A quadratic bottom drag was used for the bottom stress with the friction coefficient $C_d=3\times10^{-3}$. In a sensitivity test, the model derived with this value agreed well with the observations. The Smagorinsky equation is considered for horizontal diffusion in the model, with a coefficient recommended to be 0.2 in the POM (Blumberg and Mellor, 1987).

2.4 Model verification

Observed tidal velocity data, provided by the Third Institute of Oceanography, State Oceanic Administration of China, were used to verify the model. The modeled and observed depth-integrated magnitude and direction of velocities are seen to be in reasonable agreement (Fig.3), and the root-mean-square errors of the magnitude and direction at points P1 and P5 (Fig.1b) were 0.08 m/s and 21°, respectively.

2.5 Environmental restoration projects optimized by the model

All of the restoration projects referred to in Case 4 have been optimized and evaluated with the use of numerical modeling. As part of the Marine Environmental Restoration Project for the eastern sub-bay, we simulated 14 different project schemes, and compared and evaluated their impacts on current velocity, tidal prism, water exchange capacity, and seabed erosion-deposition intensity. Upon completion of the analysis, optimal coastline restoration and sludge dredging schemes were proposed. The proposed projects included opening Dongkeng Dike by 3 km^2 and sludge dredging to a certain level and area. In the Gaoji Dike Opening Project, the optimal size of the opening was found to be 800 m, which balances hydrodynamic improvement with project cost. In addition, sludge dredging of the nearby sea was recommended (see Case 4 in Fig.2). Numerical modeling played a critical role in confirming the restoration project implementation schemes proposed above.

3 RESULT

3.1 Tidal area

Before the analysis of the hydrodynamic changes took place, tidal areas were measured using GIS technology (Table 1). In Case 1 (1938), which had little coastal development, the tidal regions extended over 101 km^2 and 120 km^2 in the western and eastern sub-bays, respectively. During the period between Case 1 and Case 2 (1938 to 1984), a large number of coastal engineering projects (i.e., construction of dikes and land reclamation efforts) caused the tidal area to decrease rapidly by roughly 31%. In Case 3 (2007), the tidal areas had stabilized to 45 km^2 in the western sub-bay and 88 km^2 in the eastern sub-bay. From Case 1 to Case 3, this corresponds to a decreased of 55% and 27% in the western and eastern sub-bays, respectively. As mentioned in section 2, a series of restoration projects is currently underway. In Case 4 (a representation of the bay after completion of the projects), the tidal area in the western sub-bay has increased by 13 km^2 from Case 3. Although the opening of the Gaoji Dike between the western and eastern sub-bays does not increase the tidal area, it does enhance the hydrodynamic processes at work there and provides a pathway for water exchange between the two sub-bays.

3.2 Tidal current pattern

Fig.4 shows the flow pattern of the current at flood tide. The tides propagate simultaneously from the mouths of the western and eastern sub-bays. At flood tide, the outer seawater flows into the sub-bays and runs along the tidal path where the topography is eroded by strong tidal currents. The current decreases as the seafloor topography becomes shallower, moving inward from the outer part of the sub-bay. At ebb tide, the current flows out in the direction opposite to that of the flood tide. The patterns of the tidal

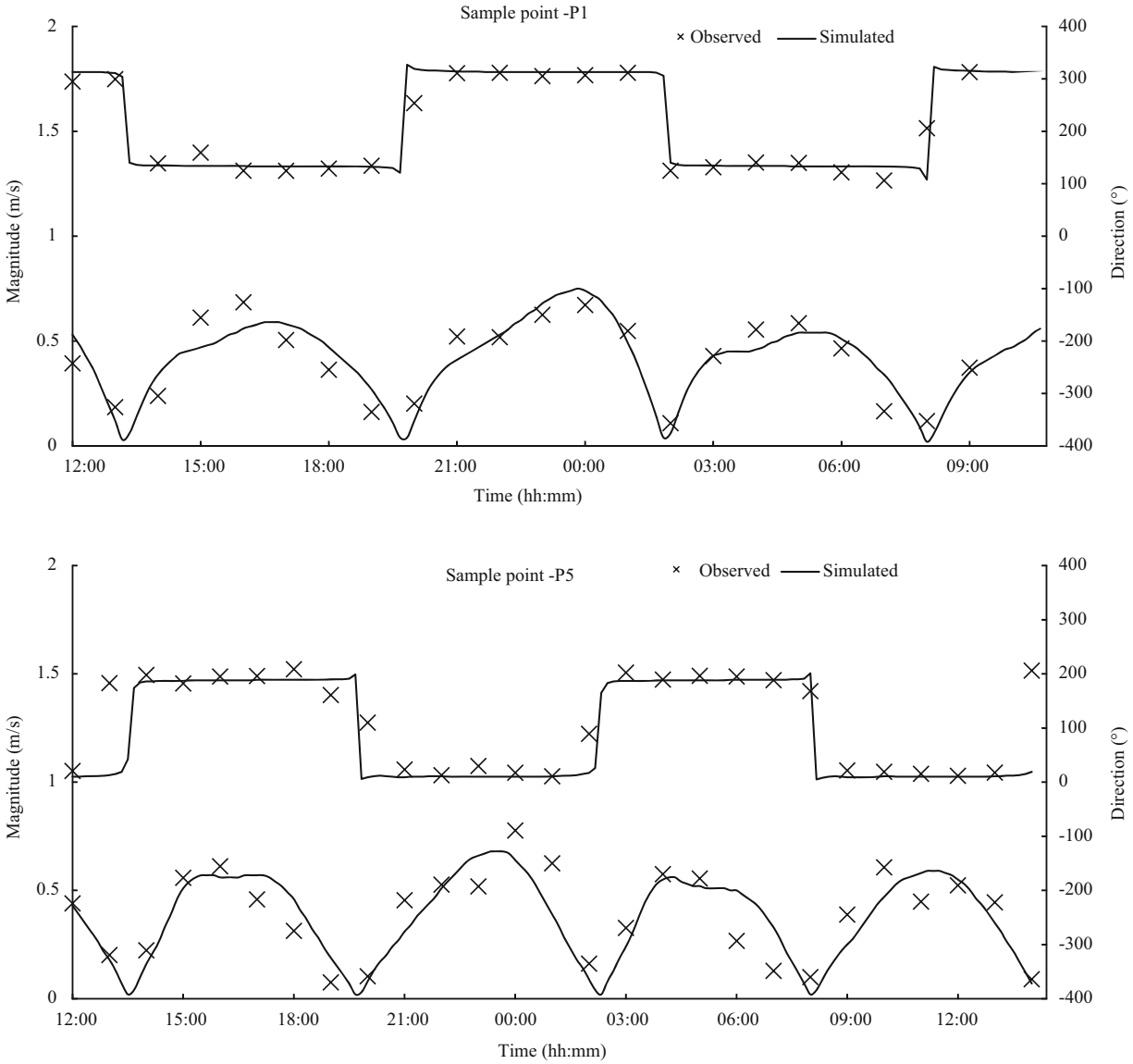

Fig.3 Velocity verification at points P1 and P5

The sample points are plotted in Fig.1b.

current in the seas are similar in all four cases, except for some local changes that are the result of the reclamations and dike construction projects.

In Case 1 (1938), the western and eastern sub-bays are connected, and the tides meet to the west of the future position of Gaoji Dike. In Cases 2 and 3 (1984 and 2007), the waters in these two sub-bays are blocked and isolated by the artificial barrier (i.e., dike). In Case 4 (2012), the tidal current from the eastern sub-bay once again flows to the west and converges with the current of the western sub-bay due to the partial opening of the dike. The waters of Maluan and Xinglin bays have resumed their exchange with outside water masses, thereby enhancing the tidal current at the mouth of the western sub-bay.

3.3 Average tidal current speed

We averaged the tidal current speed for one day (e.g., GMT+8 2007/8/14 12:00 to 2007/8/15 12:00) of the simulated spring tide. The grid points in the tidal flat area were excluded from the calculation. The averaged speeds for each of the four cases are shown in Fig.5. The figure shows that the speed in the main tidal path in Xiamen Bay is weaker in Case 2 (1984) than in Case 1 (1938). For example, high speeds (>0.7 m/s) appear at both the mouth and the middle of the western sub-bay in Case 1, but they disappear at

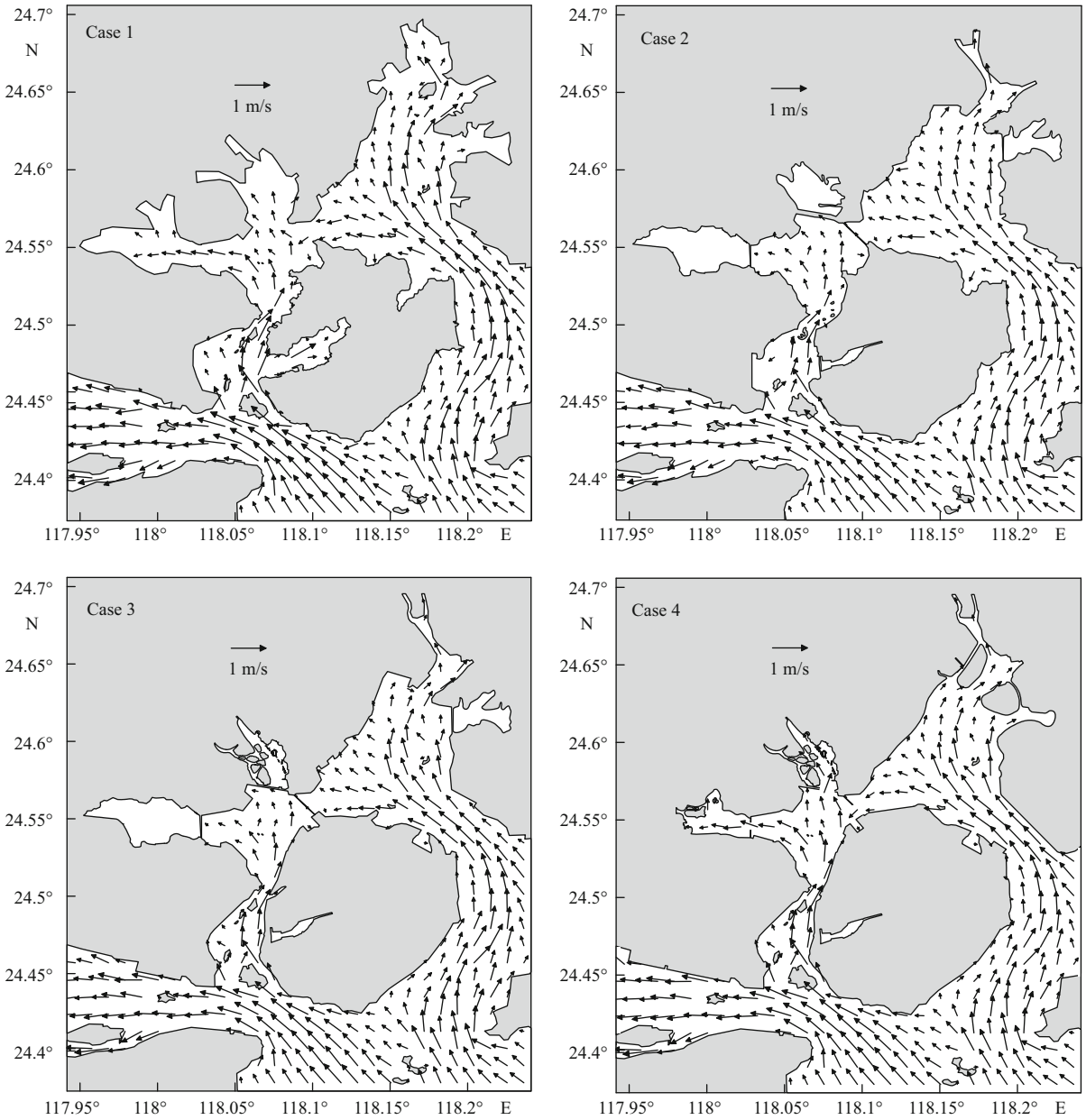

Fig.4 Velocity pattern at flood tide for the four cases

Case 1: 1938; Case 2: 1984; Case 3: 2007; Case 4: 2012

the mouths of the sub-bays in both cases 2 and 3 (1984 and 2007). The average speed decreases from 0.85 m/s to 0.55 m/s at the mouth of the western sub-bay and from 0.7 m/s to 0.55 m/s at the mouth of eastern sub-bay. The decrease in the current appears to be due to the construction of several dikes and reclamation projects between the 1950s and the 1970s. In Case 3, although the pattern of the current velocity vectors is similar to that in Case 2, the speed at the mouth of the western sub-bay decreased by 0.1 m/s, right at the location in the Xiamen harbor shipping routes where the deposition rate is the largest. After the implementation of environmental restoration projects, the speeds in both sub-bays in Case 4 (2012) increased to greater than those seen in either Cases 2 or 3. Strong currents appear at the mouths of Maluan and Xinglin bays after the opening of the dike, and the speeds at the mouths of the western and eastern sub-bays increase by more than 0.1 m/s. The greater speed in the eastern sub-bay can be attributed to the dredging project and the Dongkeng Bay opening project. The openings to Xinglin and Maluan bays critically contribute to the increased current in the western sub-bay.

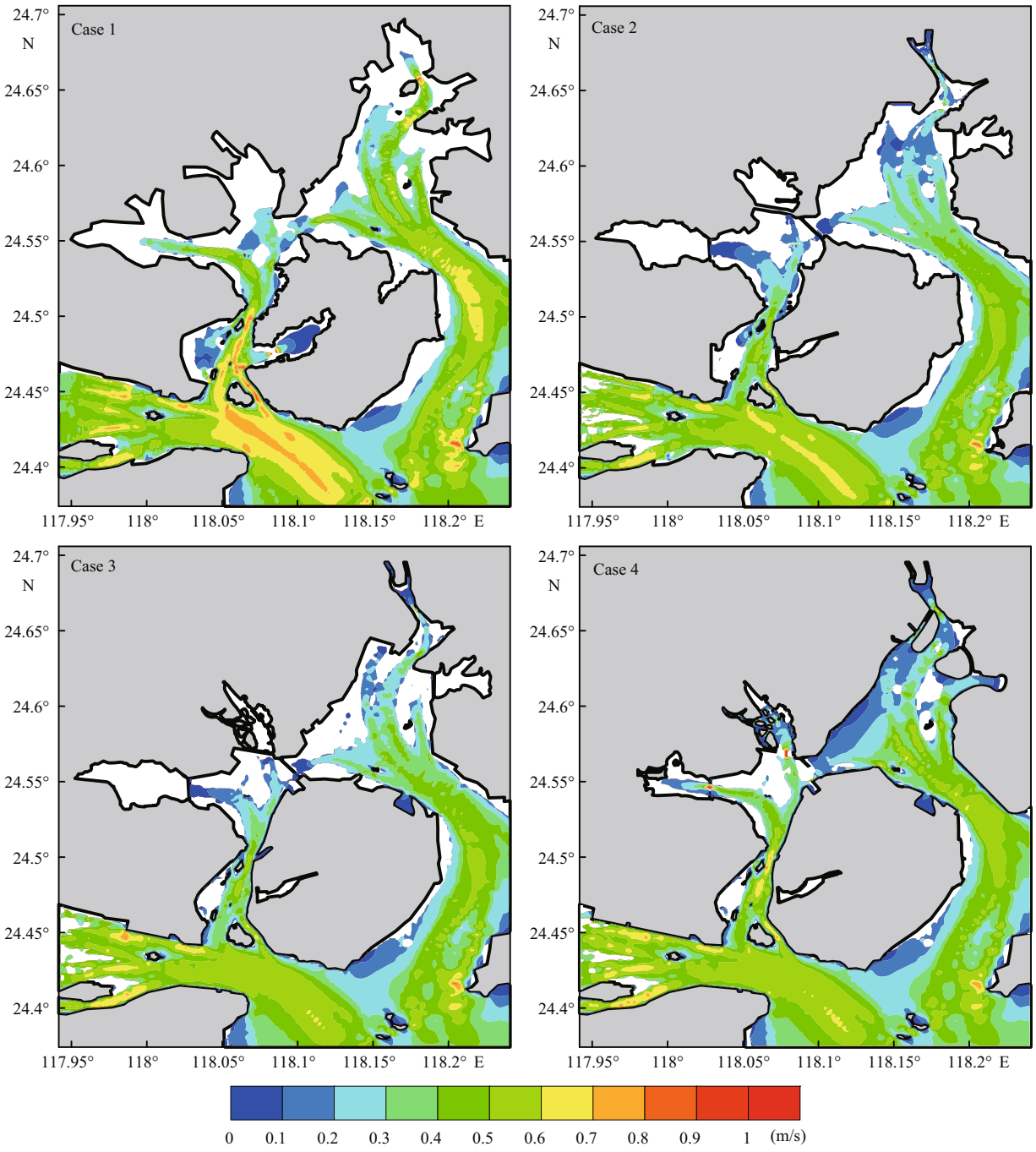

Fig.5 Average tidal current speeds for the four cases

In general, from Case 1 to Case 3 (1938 to 2007), the average tidal current speeds decreased by about 40% and 20% at the mouths of the western and eastern sub-bays, respectively. However, in Case 4 (2012), the speeds recovered to values just above those observed in Case 2 (1984). Therefore, the restoration projects appear to have caused an improvement in the tidal current.

3.4 Current speed at sample points

For quantitative analysis, six sample points were set at the mouth, middle and top of the western and eastern sub-bays, as shown in Fig.1b. The average tidal current speeds of the sample points are plotted in Fig.6 as the first hydrodynamic index. Similar to the changing tendency of the tidal area, the speeds at the

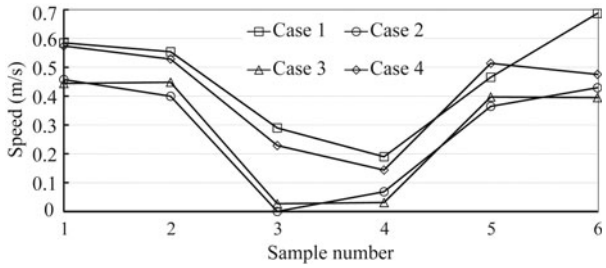

Fig.6 Average tidal current speeds at sample points for the four cases

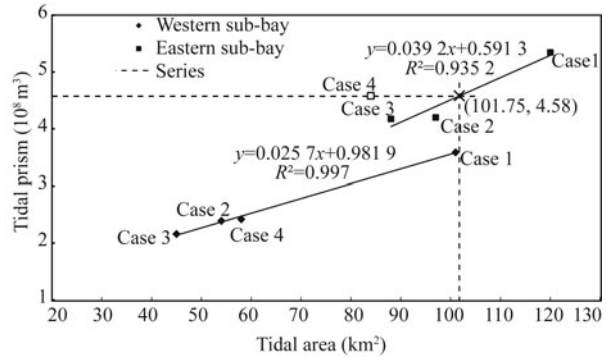

Fig.7 Linear relationship between tidal area and tidal prism in the western and eastern sub-bays

Table 2 Tidal prism statistics (unit: 10^6 m^3)

Case	S1		S2	
	Flood	Ebb	Flood	Ebb
Case 1	543	526	362	355
Case 2	426	414	242	236
Case 3	424	411	219	213
Case 4	464	452	245	239

six sample points decreased rapidly from Case 1 to Case 2 (from 1938 to 1984), experienced little change from Case 2 to Case 3 (from 1984 to 2007) and greatly increased in Case 4 (2012) as the result of the restoration projects.

During the period from Case 1 to Case 3, the speed decreased by about 20% at the mouth of the eastern sub-bay (P1) and 40% at the mouth of the western sub-bay (P6) as the tidal area decreased. In addition, the speeds at points P3 and P4 decreased to almost zero due to the building of the Gaoji Dike. The environmental restoration projects enhanced the tidal current, as indicated by the line with diamond symbols in Fig.6. Speeds at sample points P1–P5 in Case 4 increased to near to the values seen in Case 1. In the middle of the western sub-bay, where point P5 was located, the speed was even larger than that in Case 1. However, at point P6, which was located at the mouth of the western sub-bay, the speed increased only slightly more than that in Case 2. As a result, 6.7 km^2 of the lost area of the Yundang Lake cannot be recovered because of the need for flood control.

3.5 Tidal prism

Another important index of the hydrodynamics in an area is the tidal prism in a tide-dominated coastal zone. Normally, it determines the pollutant capacity and water exchange rate, and thus relates to the water quality in a bay. Two sections (S1 and S2 in Fig.1b) were set at the mouths of the eastern and western sub-bays to measure inflow and outflow water fluxes during the tidal process. The water fluxes at S1 and S2 during a tidal cycle can be defined as the tidal prisms of the eastern and western sub-bays, respectively.

Table 2 lists the details of the tidal prisms during flood and ebb tides at S1 and S2. The tidal prism decreased significantly from Case 1 to Case 2 (1938 to 1984), but decreased only slightly between Case 2 and Case 3 (1984 to 2007). Reclamation caused the tidal prism to decrease by 40% in the western sub-bay and 22% in the eastern sub-bay from Case 1 to Case 3 (1938 to 2007). After restoration construction, the tidal prism increased to 67% and 85% of the value from Case 1 in the western and eastern sub-bays, respectively. These data indicate that the tidal prism in Case 4 (2012) recovered to the conditions present at some time between those of Case 1 and Case 2.

4 DISCUSSION

Changes in the tidal area, coastline and water depth were all considered in this modeling study. We found that the hydrodynamic situation had a strong relationship with the tidal area in Xiamen Bay from Case 1 to Case 3. In other bays, a proportional relationship between tidal area and prism has been used to estimate the tidal prism (Zheng et al., 1992; Hu, 1998; Guo et al., 2007).

In conjunction with the lost tidal area, both the tidal current and tidal prism decreased by about 40% and 20% at the mouths of the western and eastern sub-bays, respectively. When the tidal area and the tidal prism of the four cases were compared (Fig.7), a high linear correlation was noted. Because the tidal prism in the eastern sub-bay increased primarily due to sludge dredging, which cannot contribute to the tidal area, the results of Case 4 were not included when

determining the linear relationship in the eastern sub-bay. The correlation coefficient between the tidal area and the tidal prism is 0.997 in the western sub-bay and 0.935 in the eastern sub-bay. The results also prove that the changes in hydrodynamic condition in the western and eastern sub-bays were caused mostly by the lost tidal area related to the reclamation works that occurred between Cases 1 and 3.

Modeling supports the forecast that restoration projects, such as the opening of the Xinglin and Maluan Dikes in the western sub-bay, will increase the tidal area in 2012 and restore it to the area measured in 1972. Similarly, because of the changes in the hydrodynamic index and the linear relationship between the tidal area and the tidal prism, we predict that the hydrodynamic status will return to the level found in 1972 in the western sub-bay upon completion of the restoration projects. For the eastern sub-bay, a special point has been marked on the trend line in Fig.7. This point indicates where the same tidal prism as that in Case 4 is found. According to the linear relationship, the value of the area at this tidal prism point is 101.75 km^2, which is equal to the value of the area in 1972. This result suggests that the sludge dredging project in the eastern sub-bay could also increase the hydrodynamic conditions to match those in 1972 (when the tidal area was approximately 101 km^2) despite the tidal area remaining the same. The effect of dredging to the marine environment was emphasized by Lee et al. (2006) in a study of Gamark Bay. In summary, we predict that after the completion of the restoration projects, the hydrodynamic status in the western and eastern sub-bays of Xiamen Bay will be restored to the levels found in 1972.

5 CONCLUSION

We have assessed the hydrodynamic changes in Xiamen Bay based on the results of a modeling study. In the early phase of coastal exploitation, reclamation and the construction of dikes helped to meet transportation and agricultural requirements by providing more land, but this lead to serious degradation of the hydrodynamic conditions in the adjacent bay. More recently, sustainable development and environmental protection have been increasingly emphasized by local authorities. Environmental restoration projects have been implemented and appear to be on the right track for the recovery of hydrodynamic conditions.

A verified two-way nested grid numerical modeling scheme was used to study the hydrodynamic changes in the western and eastern sub-bays of Xiamen Bay. Comparing the hydrodynamic indices simulated in Cases 1, 2, and 3, we conclude that the hydrodynamic conditions decreased proportionally to the tidal area in the western and eastern sub-bays because of land reclamation and dike construction activities from 1938 to 2007. During this period, the tidal current and the tidal prism both decreased by 40% in the western sub-bay and 20% in the eastern sub-bay. Through a series of environmental restoration projects proposed by experts and managers and optimized by this numerical model, the hydrodynamic environment of the near future (Case 4) is anticipated to be better than those in 1984 (Case 2). The modeling results show that the hydrodynamic state in both the western and eastern sub-bays of Xiamen Bay will increase to that seen in 1972. Nevertheless, the hydrodynamic condition will still be decreased by 33% and 15% (as compared to 1938) for western and eastern sub-bays, respectively. The results indicate that the hydrodynamic condition can be restored to some extent under a sustainable coastal development plan, although it is not possible to fully reverse the environment to that seen prior to development.

This evaluation of the changes in Xiamen Bay has been limited to the tidal current and tidal prism. However, the assessment of environmental changes in a bay is complicated and it should include more factors, such as the sediment deposition rate, water quality and ecosystem parameters. Therefore a multi-disciplinary study is needed as part of further research efforts in the area.

References

Blumberg A F, Mellor G L.1987. A description of a three-dimensional coastal ocean circulation model. *In*: Norman S H ed. Three-Dimensional Coastal Ocean Models. American Geophysical Union, Washington, D.C. p.1-16.

Chau K W. 2005. An unsteady three-dimensional eutrophication model in Tolo Harbour, Hong Kong. *Marine Pollution Bulletin*, **51**(8-12): 1 078-1 084.

Chau K W, Jiang Y W. 2001. 3D numerical model for Pearl River estuary. *J. Hydrual. Eng.*, **127** (1): 72-82.

Cheng H, Zeng W, Shi W, He H. 1985. The changes of sedimentation rate in the Xiamen Harbour since the construction of sea causeway and their implication for the ocean engineering. *Journal of Oceanography in Taiwan Strait*, **4**(1): 45-52. (in Chinese with English abstract)

Guo W, Li S, Mao L, Yin Y, Zhu D. 2007. A model for environmental impact assessment of land reclamation. *China Ocean Eng.*, **21**(2): 343-354.

Hu J. 1998. Study on sea water exchange between open sea

and Luoyuan Bay. *Marine Environment Science*, **17**: 51-54. (in Chinese with English abstract)

Jiang Y, Fang Q, Zhang L. 2004a. The effect evaluation of coastal engineering to hydrodynamics—a numerical modelling approach. *Journal of Xiamen University* (*Natural Science*), **43**(Suppl.): 263-268. (in Chinese with English abstract)

Jiang Y, Wai O W H, Hong H, Li Y. 2004b. A Geographical information system for marine management—its application in Xiamen Bay, China. *J. Coastal. Res*., **43**: 254-264.

Jiang Y, Wai O W H. 2005. Drying-wetting approach for 3D finite element sigma coordinate model for estuaries with large tidal flats. *Adv. Water Resour*., **28**(8): 779-792.

Leedertse J J. 1970. A Water Quality Simulation Model for Well-Mixed Estuaries and Coastal Seas. Vol.1, Principles of Computation. The RAND Corporation, Santa Monica, California. Report No. RM-6230-RC.

Lee M, Park S, Kang T. 2006. Influence of reclamation works on the marine environment in a semi-enclose bay. *Journal of Ocean University of China*, **5**: 219-227.

Muttil N, Chau K W. 2006. Neural network and genetic programming for modelling coastal algal blooms. *International Journal of Environment and Pollution*, **28**(3-4): 223-238.

Matsumoto K, Takanezawa T, Ooe M. 2000. Ocean tide models developed by assimilating TOPEX/POSEIDON altimeter data into hydrodynamical model: a global model and a regional model around Japan. *J. Oceanogr*., **56**: 567-581.

Oey L Y, Chen P. 1992. A nested-grid ocean model: with application to the simulation of meanders and eddies in the Norwegian coastal current. *J. Geophys. Res*., **97**(c12): 20 063-20 086.

Qin H, Ni J, Liang L. 2002 Determination of post-reclamation coastline based on hydrodynamic model. *Journal of Hydrodynamics*, **17**: 93-100. (in Chinese with English abstract)

Wu C L, Chau K W. 2006. Mathematical model of water quality rehabilitation with rainwater utilization—a case study at Haigang. *International Journal of Environment and Pollution*, **28**(3-4): 534-545.

Wang X, Sun C, Sun Y, Lou A. 2000. Study on impact of Jiaozhou Bay sea-filling on hydrodynamic environment. *Marine Environmental Science*, **19**: 55-59. (in Chinese with English abstract)

Xia H, Lin D, Niu Z. 2006. Prediction of effects of reclamation engineering on hydrodynamic conditions in the Zhanjiang Bay. *Marine Science Bulletin*, **25**: 47-54. (in Chinese with English abstract)

Xiamen Municipal Government. 2005-2008. Marine Environment Quality Report. Xiamen, China. (in Chinese)

Zhao M Y, Cheng C T, Chau K W, Li G. 2006. Multiple criteria data envelopment analysis for full ranking units associated to environment impact assessment. *International Journal of Environment and Pollution*, **28**(3-4): 448-464.

Zhao L, Wei H, Zhao J. 2002. Numerical study on water exchange in Jiaozhou Bay. *Oceanologia et Limnologia Sinica*, **33**: 23-29. (in Chinese with English abstract)

Zheng J, Zhou J, Liang J, Lin J. 2007. Hydrodynamic impact assessment of coastal reclamation project in semi-enclosed bay. *J. Coastal. Res*., **50**(Special issue): 273-276.

Zheng Q, Wu L, Dai M, Pan J, Ji Y. 1992. A remote sensing study of Jiaozhou Bay II. Calculation of dynamical parameters. *Oceanologia et Limnologia Sinica*, **23**: 1-6. (in Chinese with English abstract)